Endogenous glucocorticoids decrease skeletal angiogenesis, vascularity, hydration, and strength in 21-month-old mice

Robert S. Weinstein[1], **Chao Wan**[4], **Qinglan Liu**[4], **Ying Wang**[4], **Maria Almeida**[1], **Charles A. O'Brien**[1], **Jeff Thostenson**[2], **Paula K. Roberson**[2], **Adele L. Boskey**[3], **Thomas L. Clemens**[4], and **Stavros C. Manolagas**[1]

[1]Division of Endocrinology and Metabolism, Center for Osteoporosis and Metabolic Bone Diseases, Department of Internal Medicine, University of Arkansas for Medical Sciences, Little Rock, AR

[2]Department of Biostatistics, Central Arkansas Veterans Healthcare System, University of Arkansas for Medical Sciences, Little Rock, AR

[3]Hospital for Special Surgery, New York, NY

[4]Department of Pathology, University of Alabama at Birmingham, Birmingham, AL

Summary

Aging or glucocorticoid excess decrease bone strength more than bone mass in humans and mice, but an explanation for this mismatch remains elusive. We report that aging in C57BL/6 mice was associated with an increase in adrenal production of glucocorticoids as well as bone expression of 11β-hydroxysteroid dehydrogenase (11β-HSD) type 1, the enzyme that activates glucocorticoids. Aging also decreased the volume of the bone vasculature and solute transport from the peripheral circulation to the lacunar-canalicular system. The same changes were reproduced by pharmacologic hyperglucocorticoidism. Furthermore, mice in which osteoblasts and osteocytes were shielded from glucocorticoids via cell-specific transgenic expression of 11β-HSD type 2, the enzyme that inactivates glucocorticoids, were protected from the adverse effects of aging on osteoblast and osteocyte apoptosis, bone formation rate and microarchitecture, crystallinity, vasculature volume, interstitial fluid, and strength. In addition, glucocorticoids suppressed angiogenesis in fetal metatarsals and hypoxia inducible factor 1α transcription and VEGF production in osteoblasts and osteocytes. These results, together with the evidence that dehydration of bone decreases strength, revealed that endogenous glucocorticoids increase skeletal fragility in old age as a result of cell autonomous effects on osteoblasts and osteocytes leading to interconnected decrements in bone angiogenesis, vasculature volume, and osteocyte-lacunar-canalicular fluid.

Keywords

Aging; glucocorticoids; angiogenesis; hydraulic support; apoptosis; bone histomorphometry; osteoporosis; 11β-hydroxysteroid dehydrogenase

---

Introduction

Age-related bone loss has been an invariable feature of human biology since prehistoric times but loss of bone strength is a far more critical determinant of fracture risk than loss of bone mass (Perzigian, 1973; Hui *et al*., 1988). Endogenous or pharmacologic glucocorticoid excess also cause a decline in bone strength, and as in aging, the decline in strength with glucocorticoid excess is not only disproportional to the decline in bone mass, but precedes it in both humans and mice (Peel *et al*., 1995; Manolagas, 2000; Van Staa *et al*., 2003; Almeida *et al*., 2007a). Endogenous glucocorticoid levels increase by 20 to 50% with age in humans (Van Cauter *et al*., 1996; Dennison et al., 1999; Purnell *et al*., 2004; Reynolds *et al*., 2005) because of blunting of the glucocorticoid feedback inhibition of ACTH (Wilkinson *et al*., 2001) as well as increased bone expression of 11β-hydroxysteroid dehydrogenase (11β-HSD) type 1, the enzyme that converts glucocorticoids from inactive to active moieties (Cooper *et al*., 2002). Furthermore, cortisol concentration and the rate of bone loss are inversely related in healthy elderly men and women even after adjustments for adiposity, smoking, alcohol consumption, dietary calcium, activity, as well as serum testosterone and estradiol levels (Dennison et al., 1999; Reynolds *et al*., 2005), suggesting that endogenous glucocorticoids contribute to osteoporosis.

Bone mineral density (BMD), a surrogate measure of bone mass used routinely for clinical assessment of fracture risk, is a substantial contributor to bone strength, but other factors are also involved, including bone size, cortical and cancellous architecture, bone material properties, and osteocyte viability (Weinstein, 2000; O'Brien *et al*., 2004; Seeman, 2006). Although these alternative contributors to bone strength are well recognized, the role of skeletal water volume in the viscoelastic properties of bone has not been widely appreciated (Liebschner & Keller, 2005; Nalla *et al*., 2005; Wilson *et al*., 2006; Gennari & Bilezikian, 2009). Yet, water represents at least 25% of the wet weight of bone (Lien & Kaye, 1978; Ishijima *et al*., 1996; Prisby *et al*., 2007; Miserez *et al*., 2008) and confers to bone much of its unique strength and resilience by reducing stresses during dynamic loading and producing a 2.5-fold increase in ultimate strength (Wilson *et al*., 2006). Conversely, fracture resistance of hard tissues is defective in the absence of water (Liebschner & Keller, 2005; Nalla *et al*., 2005; Miserez *et al*., 2008). Of the total volume of water in bone, approximately 90% resides in the vasculature, marrow, and lacunar-canalicular system that surround the intricate network of osteocytes (Timmins & Wall, 1977). The remaining 10% of bone water is associated with collagen fibrils and hydroxyapatite crystals. Both aging and glucocorticoid excess cause a reduction in bone blood flow and the volume of water present in the skeleton (Lien & Kaye, 1978; Kita *et al*., 1987; Goans *et al*., 1995; Drescher *et al*., 2000; Chen et al., 2001; Prisby *et al*., 2007).

Like humans, female or male C57BL/6 mice exhibit an age-related decrease in BMD and strength in the spine and hindlimbs, and the loss of strength is detectable 9 months earlier than the loss of BMD (Almeida *et al*., 2007a). We have previously established that C57BL/6 mice also exhibit the same characteristic features of the adverse effects of pharmacologic glucocorticoid excess seen in the human skeleton (O'Brien *et al*., 2004). Here, we have used several murine models, tissues, and cells to test the hypothesis that endogenous hyperglucocorticoidism contributes to involutional osteoporosis and the mismatch between bone mass and strength that is characteristic of this condition. We have also hypothesized that the mismatch between the decrease in bone strength and mass that occurs with aging or glucocorticoid excess may be explained by loss of hydraulic support provided by the water in bone (Liebschner & Keller, 2005; Nalla *et al*., 2005; Wilson *et al*., 2006).

For some of this work, we compared wild-type C57BL/6 mice to transgenic mice overexpressing the enzyme 11β-hydroxysteroid dehydrogenase type 2 utilizing the murine

osteocalcin gene 2 (OG2) promoter, which is active only in mature osteoblasts and osteocytes (OG2-11β-HSD2 mice) (O'Brien *et al*., 2004). 11β-HSD2 inactivates both synthetic and naturally occurring glucocorticoids by oxidizing their 11β-hydroxy groups to inert 11β-keto forms, thereby preventing binding to the glucocorticoid receptor (Diederich *et al*., 2002; Sandeep & Walker, 2001). Normally, 11β-HSD2 is absent from the bones of adult mice or humans (Sher *et al*., 2004; Cooper *et al*., 2000). We have previously shown that the OG2-11β-HSD2 transgene does not affect normal bone development or turnover, as evidenced by identical bone density, strength, and histomorphometry in 5-month-old OG2-11β-HSD2 and wild-type animals and that the mice harboring the transgene are protected from the increased apoptosis of osteoblasts and osteocytes and decreased bone formation rate that occur with glucocorticoid administration (O'Brien *et al*., 2004).

We show that aging in wild type mice is associated with an increase in the adrenal production of glucocorticoids and the expression of 11β-HSD1 in bone, and that both aging and exogenous glucocorticoids decrease the volume of the bone vasculature, solute transport through the lacunar-canalicular system, and bone interstitial water, and suppress angiogenesis. Moreover, we show that the adverse effects of aging on osteoblast and osteocyte apoptosis, bone formation rate and microarchitecture, crystallinity, vasculature volume, lacunar-canalicular solute transport, and strength are attenuated in mice in which glucocorticoid action is prevented in osteoblasts and osteocytes. Furthermore, we document that glucocorticoids suppress angiogenesis in fetal metatarsals and both hypoxia inducible factor 1α (HIF1α) transcription and vascular endothelial growth factor (VEGF) production in osteoblasts and osteocytes.

Results

Endogenous glucocorticoids increase with age in mice

As a first step in determining the role of endogenous glucocorticoids in involutional osteoporosis, we measured the serum corticosterone concentrations in old and young C57BL/6 mice obtained from Harlan/NIA. The circulating corticosterone level was significantly increased in 31- as compared to 4-month-old C57BL/6 male mice (Figure 1A). To exclude the possibility that the increased corticosterone level in the older mice was due to increased excitability at the time of sampling, we measured the adrenal weight as an indication of long-term glucocorticoid production. The adrenal weight expressed per body weight was also increased in the 31- as compared to 4-month-old male animals (Figure 1B). Moreover, the vertebral expression of 11β-HSD1, a glucocorticoid activator, was increased in 25-month-old female or 31-month male C57BL/6 as compared to 4-month-old animals of either sex (Figure 1C). These data demonstrate that endogenous glucocorticoids increase in aging mice.

Age-related loss of bone mass and strength is decreased in OG2-11β-hydroxysteroid dehydrogenase type 2 mice

To investigate whether endogenous glucocorticoids contribute to the loss of BMD and strength that occurs with aging, we used a genetic model in which glucocorticoid action on osteoblasts and osteocytes is blocked via transgenic expression of 11β-HSD type 2, an enzyme that inactivates glucocorticoids before they reach the glucocorticoid receptor (OG2-11β-HSD2 mice) (O'Brien *et al*., 2004). We have previously reported that at 5-months-of-age, BMD, vertebral compression strength, osteoblast and osteocyte apoptosis, and cancellous bone histomorphometry in the wild-type and transgenic animals were not different (O'Brien *et al*., 2004), indicating that any subsequent changes due to aging are not a consequence of baseline differences. In addition, in that report, we showed that OG2-11β-HSD2 mice were protected from prednisolone-induced decreases in osteoblast number, bone

formation rate and vertebral compression strength as well from the drug-induced increases in the prevalence of osteoblast and osteocyte apoptosis (O'Brien *et al*., 2004). Body weight and vertebral size did not differ between the 21-month-old male wild-type and OG2-11β-HSD2 animals (45.2 ± 8.4 g vs. 44.0 ± 8.0 and 9.14 ± 1.13 mm^3 vs. 8.87 ± 0.83, respectively, N.S; $n = 7$ per group). The 21-month-old animals from UAMS had increased serum corticosterone levels and adrenal weight as compared with the 4-month-old mice obtained from Harlan/NIA shown in Figure 1, confirming endogenous hyperglucocorticoidism (Figure 2A). Furthermore, osteocalcin expression (the product of a glucocorticoid regulated gene) was increased in the 21-month-old OG2-11β-HSD2 mice, which also showed similar expression of 11β-HSD1 as the wild-type animals. Murine 11β-HSD2 was not detectable in either wild-type or transgenic mice and human 11β-HSD2 was only detected in the transgenic animals as expected (Sher *et al*., 2004; Cooper *et al*., 2000). Taken together, these data provide proof of principle that the human 11β-HSD2 levels were sufficient to prevent osteoblast and osteocyte increases in intracellular active glucocorticoid levels.

Between the age of 16 and 21 months, OG2-11β-HSD2 mice exhibited only 3% of the decline in vertebral BMD found in similarly aged wild-type animals (Figure 2B) and there was a trend for greater vertebral BMD at 21-months-of age (0.049 g/cm^2 ± 0.002 vs. 0.047 ± 0.003, $P = 0.09$), indicating that the age-related loss of vertebral bone mass was diminished in the transgenic mice. Moreover, the anti-aging actions of the transgene on bone resulted in an 18% greater vertebral compression strength as well as a 16% greater cancellous bone volume and 13% closer spacing as compared to the wild-type animals (Figure 2, C–E, and I). In addition, the prevalence of osteoblast and osteocyte apoptosis in the 21-month-old transgenic mice was only 47 to 57% of that in the wild-type animals (Figure 2, F, G, and L). Consistent with the findings on osteoblast apoptosis, the transgenic animals had a 36% higher bone formation rate (Figure 2, H, and L). A positive effect of the transgene was also found in the femur with a 9% greater femoral BMD (Figure 2J) and 20% greater bending strength than in the wild-type animals (Figure 2K). Therefore, these results indicate that protecting osteoblasts and osteocytes from endogenous glucocorticoids ameliorates many of the adverse effects of aging on bone.

Glucocorticoids and dehydration decrease bone strength and crystallinity in murine bone

To investigate how protecting osteoblasts and osteocytes from endogenous glucocorticoids decreased the effects of aging on bone, we first examined the relationship between BMD and strength. We determined spinal BMD *in vivo* and vertebral compression strength *ex vivo* in male and female adult Swiss-Webster mice receiving either a pharmacologic dose of prednisolone or placebo for 28 days (Figure 3A). In 148 animals receiving placebo, the relationship between bone strength and mineral density was best fit by the least squares method: stress = $-23.2 + 706.6 \times$ BMD ($r = 0.58$, $P <0.0001$). In comparison, in 47 animals receiving 2.1 mg/kg/d of prednisolone for 28 days, the relationship between bone strength and mineral density was: stress = $-43.9 + 1043 \times$ BMD ($r = 0.81$, $P < 0.0001$) and the slope of the relationship was significantly different from that found in the control animals ($P < 0.03$). When compared to the mice receiving placebo, glucocorticoids reduced bone strength by as much as one-half at the lower range of spinal BMD values. Next, we examined the relationship between vertebral ash weight and maximal load in 53 of the Swiss-Webster mice receiving placebo. In spite of a strong relationship between the two measures ($r = 0.58$, $P < 0.001$), ash weight accounted for only 34% of the maximal load (Figure 3B), indicating that the remaining 66% must be due to factors other than the amount of mineral in the bone.

To investigate the role of bone fluid on the biomechanical properties of murine bone, we determined strain (the amount of deformation tolerated before breaking) and post-yield toughness (the energy required to break the bone, a measurement of the resistance to

fracture) (Turner & Burr, 1993), in lumbar vertebrae (L6) obtained from 5-month-old and 22-month-old C57BL/6 mice, before or after vacuum drying (Figure 3C). The percent change in vertebral weight after vacuum drying was $51.8 \pm 3.0\%$ in the 5-month-old mice and $53.9 \pm 2.9\%$ in the 22-month-old mice, values not significantly different but indicating that the water content in vertebral cancellous bone and marrow is greater than that reported for bones composed of more cortical tissue (Lien & Kaye, 1978; Ishijima *et al*., 1996; Prisby *et al*., 2007; Miserez *et al*., 2008). Strain was less in hydrated vertebrae from 22-month-old C57BL/6 mice, as compared to 5-month-old animals (Figure 3D). Dehydration of L6 decreased the strain by 42% in the bones taken from the young mice, equal to the value in the relatively more brittle, hydrated bones taken from the 22-month-old mice, which showed no additional decrease in strain with drying. Drying the bones taken from the young mice also resulted in decreased energy absorbed prior to fracture as demonstrated by the 27% reduction in the post-yield toughness. There was no decrease in toughness after drying the bones taken from the 22-month-old mice, which already had lower toughness when hydrated than the bones from the young animals (Figure 3E). Because the percent change in vertebral weight after vacuum drying was not different between the bones taken from the young mice as compared to those taken from the older mice, intrinsic alterations in water localization in the older mice (e.g. more water in the marrow and less in the bone blood vessels) may be responsible for the already minimal strain and toughness. The impact of glucocorticoids on ultrastructural measures of bone structure and function was investigated by analysis of crystallinity, a measure of hydroxyapatite crystal size and perfection determined by Fourier transform infrared imaging analysis (Gourion-Arsiquaud *et al*., 2008). We used 8-month-old wild-type and OG2-11β-HSD2 mice given placebo or prednisolone for 28 days. In the wild-type animals, vertebral BMD decreased by 3.9% (5.1 ± 0.2 g/cm^2 vs. 4.9 ± 0.2, $P < 0.01$) while vertebral compression strength decreased by 29% (14.0 ± 4.2 MPa vs. 9.9 ± 2.4, $P < 0.04$). The more than 7-fold greater decrease in bone strength than in BMD is also typical of glucocorticoid-induced osteoporosis in humans (Peel *et al*., 1995; Van Staa *et al*., 2003). Vertebral crystallinity was decreased in the wild-type mice receiving prednisolone compared to those receiving placebo and this decrease was abrogated in the OG2-11β-HSD2 mice receiving prednisolone (Figure 3F). Crystallinity was lower in the placebo-treated transgenics as compared to the wild-type mice but the variance in the measurement in this group was large and the difference was not significant. Crystallinity was directly related to vertebral compression strength; 28% of the change in strength was explained by the change in crystallinity (Figure 3G). Taken together, these results suggest a strong linkage between age, glucocorticoid levels, bone hydration, crystallinity, and strength.

Glucocorticoid administration and aging decrease bone interstitial fluid

We next studied the effects of glucocorticoids and of aging on solute transport from the peripheral circulation to the lacunar-canalicular system after injection of procion red into a tail vein. Procion red fluorescence was abundant in the osteocytic lacunae and canaliculi of 8-month-old C57BL/6 male wild-type mice receiving placebo but was severely diminished after prednisolone administration (Figure 4, A, B, and C). Moreover, procion red in the osteocytelacunar-canalicular system of 25-month-old female animals was reduced by 40%, as compared to 4-month-old mice; and this decrease was detectable as early as 8 months of age (Figure 4, D, E, and F). The decrease was also found in 8- to 31-month old male mice (Figure G). The declining trend between the procion red fluorescence and months-of-age in the female and male animals was significant ($P < 0.0001$). The decrease in solute transport already apparent in the 8-month-old animal cohorts occurred at the identical time at which these same animals were previously reported to exhibit a significant decline in vertebral compression strength (Almeida *et al*., 2007a). The decline of canalicular fluorescence following prednisolone administration was ameliorated in 8-month-old OG2-11β-HSD2 transgenic mice (Figure 4C). However, there was no difference in procion fluorescence in

the placebo-treated 8-month-old wild-type and transgenic animals (Figure 4C). These results show that glucocorticoid administration and aging reduce bone interstitial fluid and that these changes were prevented by blocking glucocorticoid action on osteoblasts and osteocytes.

Glucocorticoid administration decrease bone vasculature

The effects of glucocorticoid excess on bone blood vessels were examined using µCT imaging of decalcified bone after perfusion with lead chromate. There was a decrease in vertebral and femoral vasculature in 8-month-old female C57BL/6 mice after prednisolone administration for 28 days (Figure 5, A–F). Vertebral blood vessel volume per tissue volume and surface area decreased indicating that the decrease in vasculature was due to both decreased perfusion volume and surface area available for exchange of nutrients and waste products. The decrease in vessel volume and surface area caused by glucocorticoid administration was accompanied by a decrease in the endothelial marker, von Willebrand factor, in sections of cancellous vertebral bone from mice receiving placebo and prednisolone, respectively (Figure 5, G and H). Vascular area per cancellous tissue area was reduced by an average of 74.5% with prednisolone. Taken together, these data demonstrate the adverse effects of exogenous glucocorticoids on bone vasculature.

Age-related loss of bone interstitial fluid and vascularity is prevented in OG2-11β-hydroxysteroid dehydrogenase type 2 mice

Solute transport in the lacunar-canalicular system of the 21-month-old male OG2-11β-HSD2 mice was preserved compared to the similarly aged wild-type mice (Figure 6, A and B). In the 21-month-old transgenic mice, the fluid in the osteocyte-lacunar-canalicular system was restored to the level found in the 8-month-old wild-type male animals (Figure 4C). A striking decrease in vertebral and femoral vasculature was seen in the 21-month-old C57BL/6 female wild-type mice as compared to the 8-month-old female wild-type animals receiving placebo (Figure 5 and Figure 6). The vasculature in the 21-month-old C57BL/6 wild-type female mice closely resembled that found in the 8-month-old female mice after prednisolone administration. Mice overexpressing 11β-HSD2 were protected from the effect of age on bone vasculature, as evidenced by a 74 to 115% greater vertebral and femoral vessel volume and surface area in the 21-month-old OG2-11β-HSD2 mice as compared to the wild-type controls (Figure 6, C–G). Bone vasculature in the 21-month-old transgenic mice was virtually restored to that of the 8-month-old animals. A similar decrease in immunohistostaining for von Willebrand factor in vertebral cancellous bone occurred with age and was ameliorated in the 21-month-old transgenic animals (Figure 6H). Vascular area per cancellous tissue area was increased by an average of 77.8% in the 21-month-old OG2-11β-HSD2 mice.

Glucocorticoids decrease angiogenesis, HIF1a and VEGF in osteoblasts and osteocytes

To explore the mechanism underlying our *in vivo* findings, we investigated the effects of glucocorticoid on angiogenesis and VEGF production *in vitro*, using organ and cell cultures, respectively. Dexamethasone decreased the vascular sprouting area angiogenesis in fetal metatarsal bones with or without added VEGF (Figure 7, A and B). In addition, prednisolone (or dexamethasone, data not shown) decreased tube-like structure formation by human umbilical vein endothelial cells cultured in the presence or absence of exogenous VEGF (Figure 7C). Furthermore, dexamethasone decreased both basal and desferrioxamine (DFO-a compound that augments VEGF production by inhibiting prolyl-hydroxylase)-stimulated VEGF mRNA levels and DFO-stimulated transcriptional activity of HIF1α in osteoblastic cells (Figure 7D). Likewise, dexamethasone attenuated basal (but not DFO-stimulated) VEGF mRNA levels and DFO-stimulated activity of HIF1α in an osteocytic cell line (Figure 7E). These findings suggest that the adverse effects of glucocorticoids on bone

interstitial fluid and vasculature are due to decreased angiogenesis caused by suppression of HIF1α transcription and VEGF production by osteoblasts and osteocytes themselves.

Discussion

Over the last sixty years osteoporosis has been primarily thought as a disease resulting from estrogen deficiency in both women and men (Riggs BL *et al.*, 1998). However, emerging new evidence (reviewed recently elsewhere) indicates that bone mass and strength decline with age independently of sex steroid status and that the age-related increase in oxidative stress is a fundamental mechanism of skeletal involution (Manolagas, 2010). Age-related changes in other organs and tissues, such as the ovaries, accelerate the effects of aging by decreasing defense against oxidative stress (Almeida *et al.*, 2007a). Consistent with this paradigm shift of the pathogenesis of osteoporosis, continuous defense against oxidative stress is critical for skeletal homeostasis and deletion of the FoxO transcription factors— one of the major defense mechanisms against oxidative stress— for a few weeks in young mice reproduces the adverse effects of aging on the skeleton (Ambrogini E et al., 2008). Furthermore, an age-associated diversion of β-catenin— a co-factor of Wnt signaling required for osteoblastogenesis and the suppression of adipogenesis in the bone marrow— from Wnt- to FoxO- mediated transcription of anti-oxidant gene programs may underlie the strong relationship between osteoporosis and atherosclerosis (Almeida *et al.*, 2007b; Almeida et al., 2009), and perhaps other age-related degenerative disorders including insulin resistance, hyperlipidemia, and Alzheimer's disease (Manolagas & Almeida, 2007). In agreement with the view that osteoporosis inexorably shares molecular pathogenetic mechanism related to aging per se with other degenerative disorders, ligands of the nutrient-sensing deacetylases sirtuins, are effective in the treatment of both insulin resistance and osteoporosis (Pearson *et al.*, 2008).

In the work presented here, we have elucidated yet another age-associated pathogenetic mechanism of involutional osteoporosis resulting from an increase of endogenous glucocorticoid production as well as increased sensitivity of bone cells to glucocorticoids; and, show that this mechanism may account, at least in part, for the mismatch between the decrease in bone strength and mass that occurs with both aging and glucocorticoid excess. Specifically, we found that the production of glucocorticoids in the adrenals of aging mice is increased and that the impact of this hormonal change on the aging skeleton is amplified locally because of a simultaneous increase in the bone expression of 11β-HSD type 1, the enzyme responsible for the conversion of inactive adrenal moieties to active glucocorticoids. In a manner identical to that of pharmacologic glucocorticoid excess, the age-associated increase in endogenous glucocorticoids decreased the lifespan of osteoblasts and osteocytes, the size of the vascular bed in bone, and solute transport through the lacunar-canalicular network. In agreement with the *in vivo* evidence for a suppressing effect of glucocorticoids on the bone vasculature, we obtained evidence that glucocorticoids suppress angiogenesis in cultures of fetal metatarsals. We also found that glucocorticoids suppress the transcription of HIF1α, which stimulates VEGF production and thereby decreases VEGF in osteoblasts and osteocytes as well as the action of VEGF in human umbilical vein endothelial cells.

Strikingly, shielding osteoblasts and osteocytes from endogenous glucocorticoids attenuated the adverse effects of aging on osteoblast and osteocyte apoptosis, bone formation rate and microarchitecture, crystallinity, vasculature volume, interstitial fluid, and strength, suggesting that these events are interconnected. Shielding osteoblasts and osteocytes from glucocorticoids also prevented the adverse effects of pharmacologic excess of glucocorticoids on the decrease in vasculature volume and solute transport through the lacunar-canalicular system. Collectively, these findings reveal that endogenous glucocorticoids increase skeletal fragility in old age because of cell autonomous effects on

osteoblasts and osteocytes leading to interconnected decrements in bone angiogenesis, vasculature volume, and osteocyte-lacunarcanalicular fluid. A decrease in cerebral vascularity with age has been correlated with diminished circulating insulin-like growth factor 1 (IGF-1) levels (Sonntag *et al*., 1997). In addition, the age-dependant decrease in growth hormone and IGF-1 levels is associated with increased 11β-HSD1 expression (Tomlinson *et al*., 2004). Moreover, endogenous glucocorticoids, including those generated by local increases in 11β-HSD1, have inhibitory effects on angiogenesis (Small *et al*., 2005). Therefore, glucocorticoid effects on endothelial cells are also likely to be involved in the phenomena described here. Nonetheless, the evidence that the OG2-11β-HSD2 expression in osteoblasts and osteocytes protected bone vascularity from the effects of glucocorticoids suggests that the effects on the latter two cell types must be predominant.

Bone is a dynamic organ that consists of highly specialized cells, mineralized and unmineralized connective tissue matrix, and spaces that include the bone marrow cavity, vascular canals, canaliculi, and osteocyte lacunae. Unique to bone, nutrients and oxygen are delivered by a system of tubes or channels that reaches all its cellular constituents, including the elaborate network of osteocytes – former osteoblasts buried individually within lacunae of mineralized matrix that communicate with each other and with cells on the bone surface via multiple slender cytoplasmic processes encased within canaliculi. Osteocytes and their processes in the canalicular system are surrounded by a gel-like pericellular matrix similar to the glycocalyx of endothelial cells. This matrix is in continuity with the peripheral circulation (Knothe Tate *et al*., 1998; Wang *et al*., 2005). Solute transport through the lacunar-canalicular system is accommodated in part by hydraulic vascular pressure and in part by diffusion and convection induced by mechanical loading. Transmission of fluid shear stresses to the cytoskeleton by this gel-like pericellular material is critical for the mechano-sensing function of the osteocyte network and the mechanical adaptation of bone to mechanical forces. Besides the obvious role of the bone vasculature in the supply of nutrients and oxygen, bone vascular elements are intimately linked with bone formation and repair. VEGF production by osteoblasts had been recently shown to couple osteogenesis and angiogenesis (Wang *et al*., 2007). In addition, a capillary is always present within the remodeling unit of bone and serves as the conduit of the delivery of pre-osteoclasts and pre-osteoblasts to the remodeling site (Parfitt, 2000). Moreover, endothelial cells synthesize growth factors and cytokines involved in osteogenesis (Parfitt, 2000). The findings of the present report suggest that maintenance of optimal mechanical strength through the provision of adequate solute transport and hydration is another important contribution of the vasculature to bone function. In addition to the effects on strength, diminished angiogenesis may contribute to the decrease in bone formation rate, which is typical of either aging or glucocorticoid administration (O'Brien *et al*., 2004; Almeida *et al*., 2007a).

Glucocorticoid administration in our studies caused a more than 7-fold greater decrease in bone strength than in BMD. In addition, the relationship between vertebral compression strength and spinal BMD *in vivo* was significantly different in glucocorticoid-treated animals from that found in animals receiving placebo, a finding especially prominent at the lower range of spinal BMD values. We also found that dehydration decreased the strain and energy absorbed prior to fracture in bones taken from young but not old animals. Bones taken from the old mice already had less ability to deform and absorb energy at their present state of hydration than the bones from the young hydrated animals. Protecting the osteoblasts and osteocytes from the negative effects of hyperglucocorticoidism not only prevented the negative impact of the hormones on lacunar-canalicular transport and vasculature but also prevented the decreased bone crystallinity found in the wild-type animals. Moreover, crystallinity, a measure of the size and perfection of hydroxyapatite crystals, was directly related to vertebral compression strength. It is therefore tempting to speculate that crystallinity is also compromised by the increase of endogenous

glucocorticoids that occurs with aging. Therefore, crystallinity could be another contribution to strength that cannot be detected by BMD measurements.

In support of the findings of the present report, an increase in endogenous glucocorticoids or the sensitivity of bone to these hormones evidently increases the risk of fractures in elderly patients treated with glucocorticoids for collagen vascular diseases, such as rheumatoid arthritis, (Kanis *et al.*, 2008). Thus, elderly patients (60 to 80 years-of-age) with collagen vascular diseases have a 26-fold higher risk of symptomatic vertebral fractures as compared to younger patients (18 to 31 years-of-age) following treatment with glucocorticoids (Tatsuno *et al.*, 2009). Furthermore, in this population, the interval between the initiation of glucocorticoid treatment and the occurrence of fracture becomes shorter with advancing age.

Decreased visual acuity, physical imbalance, falls, and sarcopenia are clearly risk factors for the increased fracture incidence with age as is the loss of bone mass. Nonetheless, the results of the present report establish that a decline in bone strength by itself is an inexorable accompaniment of aging. The elucidation of age-dependent molecular, cellular and tissue changes responsible for the decline of bone strength, reported herein, provides a fresh perspective into the pathogenesis of skeletal fragility with aging and suggests new therapeutic targets for its prevention—in distinction to the current alternatives which aim to alter bone mass.

Materials and Methods

Animals

Mice were electronically tagged (Biomedic Data System Inc., Maywood, NJ, USA) and kept in plastic cages (1 animal per cage) under standard laboratory conditions with a 12 hr dark, 12 hr light cycle and a constant temperature of 20° C and humidity of 48%. All mice were fed on a standard rodent diet (Agway RMH 3000, Arlington Heights, IL, USA) containing 22% protein, 5% fat, 5% fiber, 6% ash, 3.5 Kcal/g, 1.0 IU vitamin D_3/g, 0.97% calcium, and 0.85% phosphorus with water *ad libitum*. The Institutional Animal Care and Use Committee of the University of Arkansas for Medical Sciences (UAMS) approved these studies. Five- to 6-month-old Swiss Webster mice (male and female animals) were purchased from Harlan Inc. In experiments using glucocorticoid administration, we implanted slow-release pellets (Innovative Research of America, Sarasota, FL, USA) of placebo or 2.1 mg/kg/d of prednisolone for 28 days (O'Brien *et al.*, 2004). We used 4- to 25-month-old females and 4- to 31-month-old males purchased from Harlan Inc. from a cohort maintained with support from the National Institute of Aging (n = 12–15 per group) (Almeida *et al.*, 2007a). Development of OG2-11βHSD2 transgenic mice in the C57BL/6 background has been previously described (O'Brien *et al.*, 2004). We used 7- to 8-month-old and 21-month-old OG2-11βHSD2 and wild-type littermates raised at UAMS.

BMD, ashing, and bone strength measurements

Bone mineral density was measured using a QDR-1000 with customized murine software (Hologic, Inc., Bedford, MA, USA) or a PIXImus densitometer (GE-Lunar Corp., Madison, WI, USA) utilizing software version 2.0, as previously described (Almeida *et al.*, 2007a). The load bearing properties of the lumbar vertebrae L5 or L6 were measured at $37° \pm 0.5$ C using a single column material testing machine and a calibrated tension/compression load cell (Model 5542, Instron Corp., Canton, MA, USA), as previously described (O'Brien *et al.*, 2004; Almeida *et al.*, 2007a). After pre-seating with less than 0.5 Newtons (N) of applied load, vertebrae were compressed between screw-driven loading platens using a lower-platen, miniature spherical seat that minimized shear by adjusting to irregularities in the end plates of the specimens. Standard materials for compression were run before each set of

determinations. The data from four vertebrae in the placebo group compressed to failure were excluded because they did not develop the expected load-deformation or strain relationships due to slippage of the vertebrae on the lower platen. Three-point bending of the femur was done using a miniature bending apparatus with the posterior femoral surface lying on lower supports (7 mm apart) and the left support immediately proximal to the distal condyles. The bones were unnotched. Load was applied to the anterior femoral surface by an actuator midway between the two supports moving at a constant rate of 3 mm/min to produce a physiological *in vivo* strain rate of 1% for the average murine femur. Standard precision steel piano wire with stiffness in the same range as murine femoral bone was evaluated before each set of determinations. The length, width, and depth of the bones were recorded with a digital caliper at a resolution of 0.01 mm (Mitutoyo #500-196, Ace Tools, Ft. Smith, AR, USA). The mechanical properties were normalized for bone size and strength (N/mm^2; in megapascals or MPa) and toughness (the work to fracture or area under the curve of load versus strain in milliJoules or mJ) were calculated. Ashing was done in a muffle furnace at $800°$ C for 24 h in covered quartz crucibles (Fisher Scientific, Pittsburgh, PA, USA). Strain and post-yield toughness (Turner & Burr, 1993) were determined in lumbar vertebrae (L6) obtained from 5-month-old and 22-month-old C57BL/6 mice examined hydrated or after vacuum drying at $4°C$ for 50 hours.

Bone histomorphometry

The lumbar vertebrae (L1 to L4) were fixed and embedded undecalcified in methylmethacrylate and the histomorphometric examination was done on longitudinal sections using the OsteoMeasure Analysis System (OsteoMetrics, Inc., Decatur, GA, USA) as previously described (O'Brien *et al*., 2004; Almeida *et al*., 2007a). Apoptosis of osteoblasts and osteocytes was detected by in-situ end-labeling (ISEL) using the Klenow enzyme (Oncogene Research Products, Cambridge, MA, USA) in sections counterstained with 2% methyl green as previously described (O'Brien *et al*., 2004; Almeida *et al*., 2007a). Apoptotic osteoblasts were identified as cells with brown, pyknotic nuclei lining the cancellous bone perimeter and apoptotic osteocytes as brown, pyknotic cells buried in lacunae within mineralized bone (Weinstein *et al.*, 1998; Kousteni *et al.*, 2002). Vertebral cancellous bone measurements were restricted to the secondary spongiosa and cortical measurements were made at both diaphyseal cortices. Bone formation rate was defined as the distance between the double tetracycline labels multiplied by the sum of the double-labeled perimeter plus one-half of the single-labeled perimeter.

Corticosterone assay

Corticosterone was measured by RIA with a highly specific antiserum designed for use in laboratory mice (MP Biomedicals, Orangeburg, NY, USA). The detection limit was 25 ng/mL, the detection curve was linear from 25 to 500 ng/mL, and the inter-assay coefficient of variation was 6.5–7.2%. For amounts ranging from 50 to 400 ng/mL of added corticosterone, recovery was 98 to 106%. Prior to sample collection, the animals were placed in a quiet room overnight and in the morning, one cage at a time was taken for sampling. To assure that the collections represent basal corticosterone levels, all samples were obtained without anesthesia from the retro-orbital sinus within 15 seconds of gently holding the animals. Adrenal wet weight was determined immediately after necropsy and expressed as mg/g body weight.

Quantitative real-time PCR

Total mRNA was obtained from L5 using Ultraspec™ reagent (Biotecx Laboratories, Inc., Houston, Texas, USA) following instructions of the manufacturer. Equal amounts of RNA (2 μg) from each sample were reverse-transcribed using a High Capacity cDNA Archive Kit (Applied Biosystems, Forster City, CA, USA). Aliquots of the cDNA were amplified by real

time-PCR (RT-PCR) using TaqMan Universal PCR Master Mix (Applied Biosystems) on an ABI Prism 7000 Sequence Detection System (Applied Biosystems) as follows: 5-minute denaturation at 95°C for 10 min, 40 cycles of amplification including denaturation at 94°C for 15 sec and annealing/extension at 60°C for 1 min. Gene expression was calculated using the comparative threshold cycle (Ct) method using the housekeeping gene, ribosomal protein S2 (ChoB) (Almeida *et al*., 2007a). There was no significant change in ChoB with bone age. Similar results were obtained using ChoB or β-actin in the cohort of aged male animals obtained from Harlan/NIA or using ChoB, GAPDH, or β-actin in the 21-month-old wild-type and transgenic animals from UAMS.

Micro-CT

Micro-CT analysis of the distal end of the femora and the sixth lumbar vertebrae was done after the bones were dissected, cleaned, fixed in 10% Millonig's formalin and transferred to ethanol, loaded into 12.3 mm diameter scanning tubes and imaged (μCT40, Scanco Medical, Basserdorf, Switzerland). Scans were integrated into 3-D voxel images (1024 × 1024 pixel matrices for each individual planar stack). A Gaussian filter (sigma = 0.8, support = 1) was used to reduce signal noise and a threshold of 200 was applied to all analyzed scans. Scans were done at 12 μm resolution (E = 55 kVp, I = 145 μA, integration time = 200ms). The entire vertebral body was scanned with a transverse orientation excluding any bone outside the vertebral body. In the distal femur, 151 transverse slices were taken from the epicondyles and extending toward the proximal end of the femur. Manual analysis excluded the cortical bone and the primary spongiosa from the analysis. All trabecular measurements were made by manually drawing contours every 10 to 20 slices and using voxel counting for bone volume per tissue volume and sphere filling distance transformation indices without assumptions about the bone shape as a rod or plate for trabecular microarchitecture.

Fourier transform infrared imaging analysis (FTIRI)

Tissue sections (1.5–3 μm thick) of lumbar vertebrae were examined with FTIRI using a BioRad FTS infrared microscope equipped with a mercury-cadmium-telluride detector operating under nitrogen purge, and an automated x-y stage drive (BioRad, Cambridge, MA, USA). Spectra were collected from cortical bone and trabecular bone areas using a 20 μm × 20 μm aperture. Spectra of the embedding media, free of tissue, were obtained with the same aperture. Interferrograms (256 scans per data point) were collected from a minimum of six sites in three sections taken from each specimen and analyzed as previously described (Gourion-Arsiquaud *et al*., 2008). Mineral maturity or crystallinity, an index of the variation in bone crystal size and perfection as derived from x-ray diffraction line broadening analysis, was reported based on the ratio of the relative percent areas of the 1030 cm^{-1} and 1020 cm^{-1} sub-bands.

Imaging of bone vasculature

Solute transport through the lacunar-canicular system was visualized using procion red MX-5B (Sigma-Aldridge, St. Louis, MO, USA), a 200–300 molecular weight fluorescent tracer, which was injected into the tail vein of anesthetized mice using a 0.8% aqueous solution (0.01 mL/g body weight at 0.1 mL/min). In preliminary experiments, mice were sacrificed at various intervals after injection to determine the time required for maximal filling of the lacunar-canicular system independently of the perfusion rate through bone. Filling of the system could be seen as early as 5 minutes after injection and fading of the procion signal occurred by 20 minutes so necropsy was done 15 minutes after injection. Lumbar vertebrae L1–4 were prepared for embedding in methyl methacrylate. Three mice were injected from each group, 3 nonconsecutive sections were taken from each mouse, and 3 photomicrographs were made from each section. Quantification of the procion red in the osteocyte-lacunar-canicular system of the cancellous bone was by image analysis using

photomicrographs taken with structured epifluorescent illumination obtained by means of a tomographic grid projection technique (Zeiss Apotome system, Carl Zeiss, Inc., Thornwood, NY, USA) and analyzed by Image-Pro Plus software (Media Cybernetics, Silver Springs, MD, USA).

The bone vascular bed was visualized after flushing the vasculature with heparinized saline (0.9% N) followed by 10% Millonig's formalin and perfusing with a radiopague lead chromate silicone rubber compound (Microfil MV-122, Flow Tech, Carver, MA, USA) by IV drip through the left ventricle until it passed through the systemic vasculature and exuded from the inferior vena cava (Wang *et al*., 2007). Animals were then stored at 4°C for 24 h to complete polymerization of the compound (n = 5 per group). Lumbar vertebrae (L5) and femora were fixed in 10% Millonig's formalin for 24 h and decalcified in formic acid (Cal Ex II, Fisher Scientific, Pittsburg, PA, USA) for 24–48 h. After transfer to 70% ethanol, μCT imaging was done at medium resolution (14 μm isotropic voxel size) using a threshold of 308. The primary measurements were tissue volume, vascular volume, and vascular surface area. Vascular volume per tissue volume was calculated.

Immunohistochemical staining procedure

Mounted slides sectioned from methylmethacrylate-embedded bone blocks were deplasticized using 2-methoxyethyl acetate (Sigma Aldrich, Saint Louis, MO, USA) and 95%, 80%, 70% alcohol and then transferred to distilled water. Antigen retrieval was done at 48°C for 4 minutes in 10 mM citrate buffer (Thermo Fisher Scientific, Houston, TX, USA) after which the slides were rinsed and exposed to 3% alcoholic H_2O_2 (Sigma Aldrich) for five minutes to quench endogenous peroxidase, rinsed again and introduced to phosphate-buffered saline (PBS, Diamedix Corp, Miami, FL, USA). Slides were then flooded with normal horse serum (RTU VectaStain Kit, Vector Labs, Burlingame, CA, USA) for 20 minutes at room temperature, drained and diluted primary antibody for von Willebrand factor (Dako A0082, Denmark) was applied to each. Negative controls had the antibody diluent applied without the antibody. Incubation was two hours at 37°C. Slides were then rinsed in PBS and exposed to biotinylated universal anti-rabbit/mouse IgG for 30 minutes at room temperature followed by another rinse in PBS and exposure to RTU ABC reagent for 30 minutes. After another rinse in PBS, the slides were treated with DAB (EMD Biosciences, San Diego, CA, USA) for two minutes, flooded with 0.15% copper sulfate in 0.9% Saline solution (Thermo Fisher, USA) for two minutes, exposed to 1.0% methyl green (Sigma Aldrich) for two minutes and then cover slips were applied. Vascular area per cancellous tissue area and excluding the cancellous bone was analyzed by Image-Pro Plus software (Media Cybernetics, Silver Springs, MD, USA)

Fetal mouse metatarsal angiogenesis assay

E17.5 embryos were removed from timed-pregnancy mice and metatarsals were dissected and cultured in 24-well plates in 150 ul of α-modified Eagle's medium with 10% heat-inactivated FBS and 1% penicillin/streptomycin for 72 hours as described (Wang *et al*., 2007). Medium was replaced and the bones cultured for 14 days with vehicle or DEX at 10^{-10}, with and without the addition of 10 ng/mL of VEGF, and with medium replacements every 3 days (n = 6 for each group). Explants were fixed in zinc formalin for 15 minutes at room temperature and stained for CD31 (BD Biosciences, Pharmingen, USA). The assay was done in triplicate. Photomicrographs were taken with a stereomicroscope and digital camera (Discovery V12 and AxioCam, Carl Zeiss, Inc., Thornwood, NY, USA) and analyzed by Image-Pro Plus software (Media Cybernetics, Silver Springs, MD, USA).

Human umbilical vein endothelial cell assay

The effect of prednisolone on angiogenesis was examined *in vitro* with a Matrigel angiogenesis assay using human umbilical vein endothelial cells (Wang *et al.*, 2007). The cells were cultured on Matrigel chambers with or without prednisolone. The addition of 10 ng/mL of VEGF or10 nM sulforaphane served as positive and negative controls. Sulforaphane is an isothiocyanate derivative that inhibits angiogenesis via suppression of endothelial cell proliferation. The number of tube-like structures was quantified after 12 hours in culture.

Glucocorticoid effects on OB6 and MLO-Y4 cells

Desferrioxamine (DFO) (25 μM) was purchased from Sigma-Aldrich (St. Louis, MO, USA). The HIF1α-responsive luciferase reporter construct (HRE-Luc) containing three hypoxic response element sites was obtained from N. S. Chandel (Northwestern University Medical School, Chicago, IL, USA). OB-6 osteoblastic cells were cultured in α-modified Eagle's medium supplemented with 10% FBS and 1% each of penicillin, streptomycin, and glutamine. MLO-Y4 osteocytic cells were cultured as previously described (Plotkin *et al.*, 1999). Cells were cultured with vehicle or DEX at 10^{-8}. Plasmid constructs were introduced into cells by transient transfection using Lipofectamine Plus (Invitrogen, Carlsbad, CA, USA). Cells were plated in 48 well plates and transfected 16 h later with a total of 0.4 μg of DNA. Luciferase activity assay was performed using a Dual luciferase assay kit (Promega, Madison, WI, USA) as described by the manufacturer.

Statistics

To investigate treatment effects for the various measurements, one-way ANOVA was used. All pairwise comparisons were analyzed using the Bonferroni correction for multiple comparisons (SAS/STAT, 2002; StatCorp, 2005). A generalized linear model was used to fit and compare the regression lines of stress vs. BMD for control animals and mice receiving prednisolone. The coefficient of determination (r^2) was used to evaluate the amount of variation in the dependent variable that can be accounted for by changes in the predictor variable. The data are represented as the mean ± standard deviations (SD).

Acknowledgments

References

Almeida M, Han L, Martin-Millan M, Plotkin LI, Stewart SA, Roberson PK, Kousteni S, O'Brien CA, Bellido T, Parfitt AM, Weinstein RS, Jilka RL, Manolagas SC. Skeletal involution by age-associated oxidative stress and its acceleration by loss of sex steroids. J. Biol. Chem. 2007a; 282:27285–27297. [PubMed: 17623659]

Almeida M, Han L, Martin-Millan M, O'Brien CA, Manolagas SC. Oxidative stress antagonizes Wnt signaling in osteoblast precursors by diverting beta-catenin from T cell factor- to forkhead box O-mediated transcription. J. Biol. Chem. 2007b; 282:27298–27305. [PubMed: 17623658]

Almeida M, Ambrogini E, Han L, Manolagas SC, Jilka RL. Increased lipid oxidation causes oxidative stress, increased PPAR{gamma} expression and diminished proosteogenic Wnt signaling in the skeleton. J. Biol. Chem. 2009 doi: 10.1074/jbc.M109.023572.

Ambrogini E, O'Brien CA, Martin-Millan M, Paik J, DePinho RA, Han L, Warren A, Shelton RS, Qui X, Goellner JJ, Jilka RL, Almeida M, Manolagas SC. Loss or Gain of FoxO Function in Osteoclasts and Osteoblasts Alters the Rate of Apoptosis and BMD in Mice. J. Bone. Min. Res. 2008; 23:S70.

Chen W-T, Shih TT, Chen R-C, Lo S-Y, Chou C-T, Lee J-M, Tu H-Y. Vertebral bone marrow perfusion evaluated with dynamic contrast-enhanced MR imaging: significance of aging and sex. Radiology. 2001; 220:213–218. [PubMed: 11426000]

Cooper MS, Walker EA, Bland R, Fraser WD, Hewison M, Stewart PM. Expression and functional consequences of 11β-hydroxysteroid dehydrogenase activity in human bone. Bone. 2000; 27:375–381. [PubMed: 10962348]

Cooper MS, Rabbitt EH, Goddard PE, Bartlett WA, Hewison M, Stewart PM. Osteoblastic 11beta-hydroxysteroid dehydrogenase type 1 activity increases with age and glucocorticoid exposure. J. Bone Miner. Res. 2002; 17:979–986. [PubMed: 12054173]

Dennison E, Hindmarsh P, Fall C, Kellingray S, Barker D, Phillips D, Cooper C. Profiles of endogenous circulating cortisol and bone mineral density in healthy elderly men. J. Clin. Endocrinol. Metab. 1999; 84:3058–3063. [PubMed: 10487665]

Diederich S, Ekkehard E, Burkhardt P, Quinkler M, Bumke-Vogt C, Rochel M, Seidelmann D, Esperling P, Oelkers W, Bähr V. 11β-hydroxysteriod dehydrogenase types 1 and 2: an important pharmacokinetic determinant for the activity of synthetic mineralo- and glucocorticoids. J Clin Endocrinol Metab. 2002; 87:5695–5701. [PubMed: 12466373]

Drescher W, Li H, Qvesel D, Jensen SD, Flo C, Hansen ES, Bünger C. Vertebral blood flow and bone mineral density during long-term corticosteroid treatment: An experimental study in immature pigs. Spine. 2000; 25:3021–3025. [PubMed: 11145813]

Gennari L, Bilezikian JP. Glucocorticoid-induced osteoporosis: hope on the horizon. Lancet. 2009; 373:1225–1226. [PubMed: 19362657]

Goans RE, Weiss GH, Abrams SA, Perez MD, Yergey AL. Calcium tracer kinetics show decreased irreversible flow to bone in glucocorticoid treated patients. Calcif. Tissue Int. 1995; 56:533–535. [PubMed: 7648481]

Gourion-Arsiquaud S, West PA, Boskey AL. Fourier transform-infrared microspectroscopy and microscopic imaging. Methods Mol. Biol. 2008; 455:293–303. [PubMed: 18463826]

Hui SL, Slemenda CW, Johnston CC. Age and bone mass as predictors of fracture in a prospective study. J. Clin. Invest. 1988; 81:1804–1809. [PubMed: 3384952]

Ishijima H, Ishizaka H, Horikoshi H, Sakurai M. Water fraction of lumbar vertebral bone marrow estimated from chemical shift misregistration on MR imaging. Am. J. Roentgenol. 1996; 167:355–358. [PubMed: 8686603]

Kanis JA, Johnell O, Johansson H, McCloskey E. FRAX and the assessment of fracture probability in men and women from the UK. Osteoporos. Int. 2008; 19:385–397. [PubMed: 18292978]

Kita K, Kawai K, Hirohata K. Changes in bone marrow blood flow with aging. J. Orthop. Res. 1987; 5:569–575. [PubMed: 3681531]

Knothe Tate ML, Niederer P, Knothe U. In vivo tracer transport through the lacunocanalicular system of rat bone in an environment devoid of mechanical loading. Bone. 1998; 22:107–117. [PubMed: 9477233]

Kousteni S, Chen JR, Bellido T, Han L, Ali AA, O'Brien CA, Plotkin L, Fu Q, Mancino AT, Wen Y, Vertino AM, Powers CC, Stewart SA, Ebert R, Parfitt AM, Weinstein RS, Jilka RL, Manolagas SC. Reversal of bone loss in mice by nongenotropic signaling of sex steroids. Science. 2002; 298:843–846. [PubMed: 12399595]

Liebschner MAK, Keller TS. Hydraulic strengthening affects the stiffness and strength of cortical bone. Ann. Biomed. Eng. 2005; 33:26–38. [PubMed: 15709703]

Lien J, Kaye M. Changes in the red cell, plasma, and inulin spaces and in the total water contents of rat femurs in cortisone induced osteoporosis. Calc. Tiss. Res. 1978; 25:245–248.

Manolagas SC. Corticosteroids and fractures: a close encounter of the third cell kind. J. Bone Miner. Res. 2000; 15:1001–1005. [PubMed: 10841168]

Manolagas SC, Almeida M. Gone with the Wnts: beta-catenin, T-cell factor, forkhead box O, and oxidative stress in age-dependent diseases of bone, lipid, and glucose metabolism. Mol. Endocrinol. 2007; 21:2605–2614. [PubMed: 17622581]

Manolagas SC. From Estrogen-centric to Aging and Oxidative Stress: A Revised Perspective of the Pathogenesis of Osteoporosis. Endo. Rev. 2010 In Press.

Miserez A, Schneberk T, Sun C, Zok FW, Waite JH. The transition from stiff to compliant material in squid beaks. Science. 2008; 319:1816–1819. [PubMed: 18369144]

Nalla RK, Balooch M, Ager JW, Kruzic JJ, Kinney JH, Ritchie RO. Effects of polar solvents on the fracture resistance of dentin: role of water hydration. Acta. Biomater. 2005; 1:31–43. [PubMed: 16701778]

O'Brien CA, Jia D, Plotkin LI, Bellido T, Powers CC, Stewart SA, Manolagas SC, Weinstein RS. Glucocorticoids act directly on osteoblasts and osteocytes to induce their apoptosis and reduce bone formation and strength. Endocrinol. 2004; 145:1835–1841.

Parfitt AM. The mechanism of coupling: a role for the vasculature. Bone. 2000; 26:319–323. [PubMed: 10787232]

Pearson KJ, Baur JA, Lewis KN, Peshkin L, Price NL, Labinskyy N, Swindell WR, Kamara D, Minor RK, Perez E, Jamieson HA, Zhang Y, Dunn SR, Sharma K, Pleshko N, Woollett LA, Csiszar A, Ikeno Y, Le Couteur D, Elliott PJ, Becker KG, Navas P, Ingram DK, Wolf NS, Ungvari Z, Sinclair DA, de Cabo R. Resveratrol delays age-related deterioration and mimics transcriptional aspects of dietary restriction without extending life span. Cell. Metab. 2008; 8:157–168. [PubMed: 18599363]

Peel NFA, Moore DJ, Barrington NA, Bax DE, Eastell R. Risk of vertebral fracture and relationship to bone mineral density in steroid treated rheumatoid arthritis. Ann. Rheum. Dis. 1995; 54:801–806. [PubMed: 7492217]

Perzigian AJ. Osteoporotic bone loss in two prehistoric Indian populations. Am. J. Phys. Anthropol. 1973; 39:87–95. [PubMed: 4351578]

Plotkin LI, Weinstein RS, Parfitt AM, Manolagas SC, Bellido T. Prevention of osteocyte and osteoblast apoptosis by bisphosphonates and calcitonin. J. Clin. Invest. 1999; 104:1363–1374. [PubMed: 10562298]

Prisby RD, Ramsey MW, Behnke BJ, Dominguez JM, Donato AJ, Allen MR, Delp MD. Aging reduces skeletal blood flow, endothelium-dependent vasodilatation, and NO bioavailability in rats. J. Bone Miner. Res. 2007; 22:1280–1288. [PubMed: 17451371]

Purnell JQ, Brandon DD, Isabelle LM, Loriaux DL, Samuels MH. Association of 24-hour cortisol production rates, cortisol-binding globulin, and plasma-free cortisol levels with body composition, leptin levels, and aging in adult men and women. J. Clin. Endocrinol. Metab. 2004; 89:281–287. [PubMed: 14715862]

Reynolds RM, Dennison EM, Walker BR, Syddall HE, Wood PJ, Andrew R, Phillips DI, Cooper C. Cortisol secretion and rate of bone loss in a population-based cohort of elderly men and women. Calcif. Tissue Int. 2005; 77:134–138. [PubMed: 16151676]

Riggs BL, Khosla S, Melton LJ III. A unitary model for involutional osteoporosis: estrogen deficiency causes both type I and type II osteoporosis in postmenopausal women and contributes to bone loss in aging men. J. Bone. Miner. Res. 1998; 13:763–776. [PubMed: 9610739]

Sandeep TC, Walker BR. Pathophysiology of modulation of local glucocorticoid levels by 11β-hydroxysteroid dehydrogenases. Trends in Endocrinol. Metab. 2001; 12:446–453. [PubMed: 11701343]

SAS/STAT. SAS Institute Inc. version 9.1. SAS Institute Inc.; Cary, NC: 2002.

Seeman E. Bone quality – the material and structural basis of bone strength and fragility. N. Engl. J. Med. 2006; 354:2250–2261. [PubMed: 16723616]

Sher LB, Woitge HW, Adams DJ, Gronowicz GA, Krozowski Z, Harrison JR, Kream BE. Transgenic expression of 11β-hydroxysteroid dehydrogenase type 2 in osteoblasts reveals an anabolic role for endogenous glucocorticoids in bone. Endocrinol. 2004; 145:922–929.

Small GR, Hadoke PWF, Sharif I, Dover AR, Armour D, Kenyon CJ, Gray GA, Walker BR. Preventing local regeneration of glucocorticoids by 11β-hydroxysteroid dehydrogenase type 1 enhances angiogenesis. Proc. Natl. Acad. Sci. USA. 2005; 102:12165–12170. [PubMed: 16093320]

Sonntag WE, Lynch CD, Cooney PT, Hutchins PM. Decreases in cerebral microvasculature with age are associated with the decline in growth hormone and insulin-like growth factor 1. Endocrinol. 1997; 138:3515–3520.

StatCorp. Stata statistical software: release 8.2. Stata Corp; College Station, TX: 2005.

Tatsuno I, Sugiyama T, Suzuki S, Yoshida T, Tanaka T, Sueishi M, Saito Y. Age dependence of early symptomatic vertebral fracture with high-dose glucocorticoid treatment for collagen vascular diseases. J. Clin. Endocrinol. Metab. 2009; 94:1671–1677. [PubMed: 19258412]

Timmins PA, Wall JC. Bone water. Calc. Tiss. Res. 1977; 23:1–5.

Tomlinson JW, Walker EA, Bujalska IJ, Draper N, Lavery GG, Cooper MS, Hewison M, Stewart PM. 11β-hydroxysteroid dehydrogenase type 1: a tissue specific regulator of glucocorticoid response. Endo. Rev. 2004; 25:831–866.

Turner CH, Burr DB. Basic biomechanical measurements of bone: a tutorial. Bone. 1993; 14:595–608. [PubMed: 8274302]

Van Cauter E, Leproult R, Kupfer DJ. Effects of gender and age on the levels and circadian rhythmicity of plasma cortisol. J. Clin. Endocrinol. Metab. 1996; 81:2468–2473. [PubMed: 8675562]

Van Staa TP, Laan RF, Barton IP, Cohen S, Reid DM, Cooper C. Bone density threshold and other predictors of vertebral fracture in patients receiving oral glucocorticoid therapy. Arth. Rheum. 2003; 48:3224–3229. [PubMed: 14613287]

Wang L, Wang Y, Han Y, Henderson SC, Majeska RJ, Weinbaum S, Schaffler MB. In situ measurement of solute transport in the bone lacunar-canalicular system. Proc. Natl. Acad. Sci. U S A. 2005; 102:11911–11916. [PubMed: 16087872]

Wang Y, Wan C, Deng L, Liu X, Cao X, Gilbert SR, Bouxsein ML, Faugere MC, Guldberg RE, Gerstenfeld LC, Haase VH, Johnson RS, Schipani E, Clemens TL. The hypoxia-inducible factor alpha pathway couples angiogenesis to osteogenesis during skeletal development. J. Clin. Invest. 2007; 117:1616–1626. [PubMed: 17549257]

Weinstein RS, Jilka RL, Parfitt AM, Manolagas SC. Inhibition of osteoblastogenesis and promotion of apoptosis of osteoblasts and osteocytes by glucocorticoids: potential mechanisms of the deleterious effects on bone. J. Clin. Invest. 1998; 102:274–282. [PubMed: 9664068]

Weinstein RS. Perspective: True strength. J. Bone Miner. Res. 2000; 15:621–625. [PubMed: 10780853]

Wilkinson CW, Petrie EC, Murray SR, Colasurdo EA, Raskind MA, Peskind ER. Human glucocorticoid feedback inhibitions reduced in older individuals: evening study. J. Clin. Endocrinol. Metab. 2001; 86:545–550. [PubMed: 11158007]

Wilson EE, Awonusi A, Morris MD, Kohn DH, Tecklenburg MM, Beck LW. Three structural roles for water in bone observed by solid-state NMR. Biophys. J. 2006; 90:3722–3731. [PubMed: 16500963]
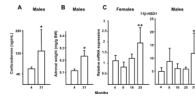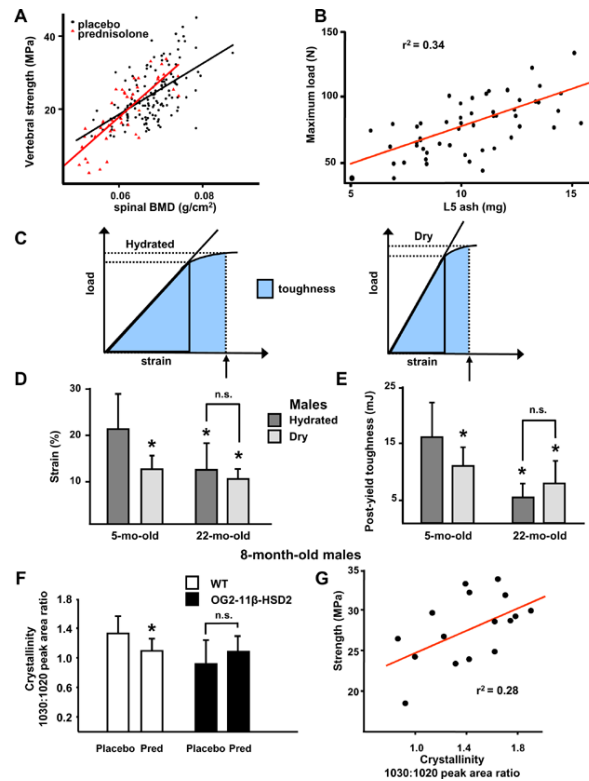
Figure 1.
C57BL/6 mice from a cohort at Harlan Inc. maintained by NIA exhibit an increase in endogenous glucocorticoid production and activation with age. Increased serum corticosterone ($n = 3$ to 9 per group) (**A**) and adrenal weight ($n = 10$ to 12 per group) (**B**) from 4- to 31-month-old male mice are shown. Vertebral 11β-HSD1 expression in 4- to 25-month-old female mice ($n = 10$ to 12 per group) and in 4- to 31-month old male mice ($n = 3$ to 9 per group) (**C**) also increased with age. There was no significant change in ChoB with bone age. Data represent the mean ± SD. * $P < 0.05$ vs. 4-month-old mice, ** $P < 0.005$ vs. 4-month-old mice.
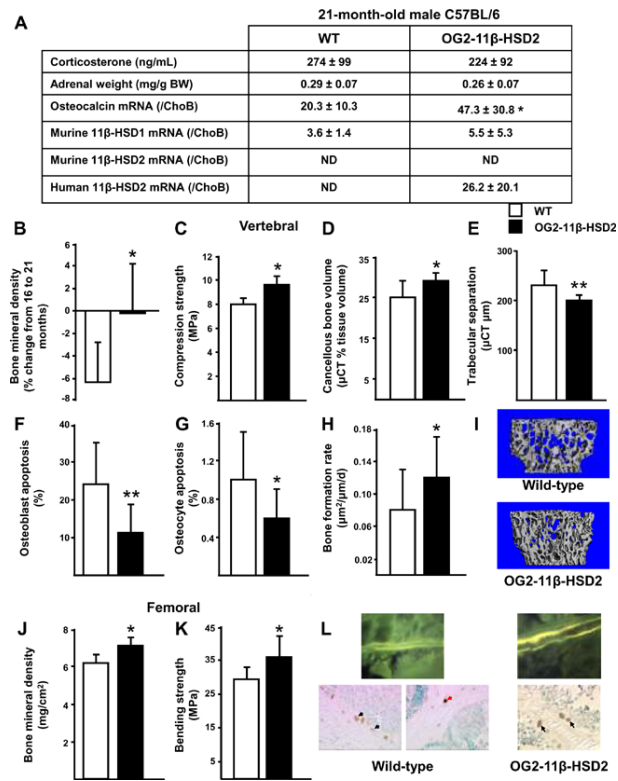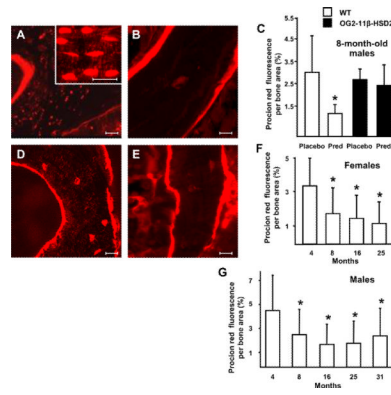
Figure 2.
Preservation of bone density, strength, microarchitecture, osteoblast and osteocyte apoptosis, and formation rate in 21-month-old OG2-11β-HSD2 mice developed on a C57BL/6 background, bred, and maintained at UAMS (OG2-11β-HSD2, black bars) as compared to wild-type mice also maintained at UAMS (WT, white bars). Earlier development of endogenous hyperglucocorticoidism in the mice raised at UAMS as compared to those from the Harlan/NIA source is documented by the corticosterone levels, adrenal weights, and relative osteocalcin expression data. The expression of 11β-HSD1 in the wild-type and transgenic animals was similar. Murine 11β-HSD2 was not detectable in either wild-type or transgenic mice and human 11β-HSD2 was only detected in the transgenic animals as expected. (**A**), comparisons of the change in vertebral BMD from 16 to 21 months-of-age (**B**), compression strength (**C**), μCT determinations of bone volume/ tissue volume, trabecular separation, and representative μCT images of bone (**D, E, I**), osteoblast and osteocyte apoptosis (**F, G**), bone formation rate (**H**), femoral BMD at 21 months-of-age (**J**), femoral bending strength (**K**), and representative photomicrographs of bone formation and apoptosis (**L**) are shown. Black arrows indicate the brown, ISEL-positive, apoptotic osteoblasts located at the cancellous bone perimeter and red arrows indicate apoptotic osteocytes are buried in lacunae within mineralized bone. Data represent the mean ± SD. ND, not detectable, * P <0.05, ** P <0.02. (n = 6 to 11 per group).
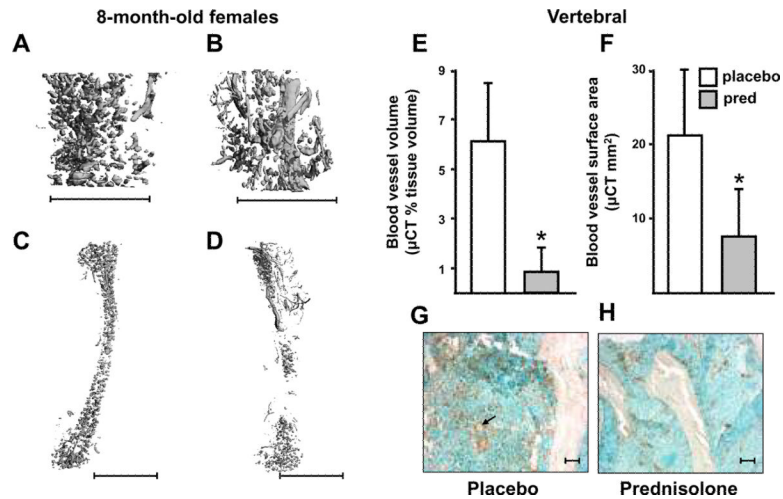
Figure 3.
Glucocorticoids decrease bone strength more than BMD. Normalized for bone size, vertebral compression strength (N/mm^2 or MPa) and BMD (g/cm^2) were measured in male and female Swiss Webster mice, aged 5 to 6 months and given placebo (black circles, $n = 148$) or prednisolone (red triangles, $n = 47$) for 28 days (**A**). The relationship between vertebral ash weight (mg) and maximal load (N) in 53 of the Swiss Webster placebo control mice from (**A**) is shown in (**B**). The relationships between the measurements of load, strain and toughness (the area under the load/strain curve) before and after vacuum drying are shown in (**C**). (**D, E**) Water contributes to fracture resistance in young but not old C57BL/6 male mice as measured by bone strain or deformation (**D**) and bone toughness or resistance to fracture (**E**). Dark gray bars are hydrated and light gray bars are vacuum dried vertebrae. ($n = 12$ to 15 per group; * $P < 0.05$ vs. the hydrated 5-month-old group; n.s., not significant). (**F, G**) Fourier transform infrared imaging analysis in 8-month-old male wild-type (white bars) and OG2-11β-HSD2 transgenic mice (black bars) given placebo or prednisolone for 28 days. Crystallinity, the ratio of the relative areas of the 1030 and 1020 cm-1 peaks, decreased in wild-type but not in OG2-11β-HSD2 mice (* $P < 0.05$, $n = 8$ to 9 per group) (**F**). Vertebral compression strength and crystallinity were directly related (**G**). (r$^2 = 28\%$, $r = 0.53$, $P < 0.03$, $n = 4$ from each group). Data are given as the mean ± SD.
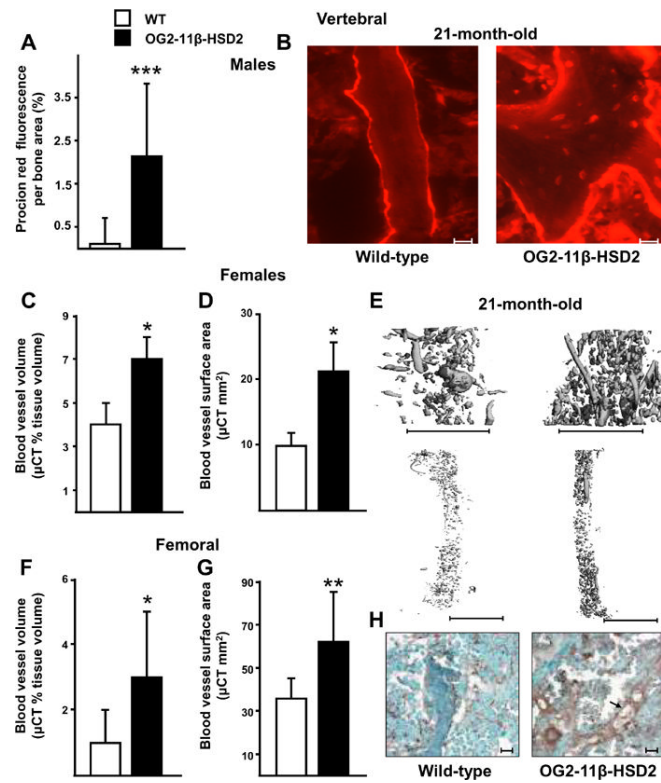
Figure 4.
Prednisolone administration or aging decrease solute transport through the vertebral lacunarcanalicular system. Procion red fluorescence per cancellous bone area decreased after 28 days of prednisolone administration to 8-month-old male wild-type (WT, white bars) but this effect was blocked in the OG2-11β-HSD2 mice (black bars) (**A-C**). Eight-month-old WT and OG2-11β-HSD2 mice receiving placebo had similar procion fluorescence. Scale bars: 10 um. Procion red fluorescence decreased from 4- to 25-months-of-age in female C57BL/6 mice (**D-F**) and in 4- to 31-month-old males (**G**). Representative photomicrographs are shown. Data represent the mean ± SD. (* $P < 0.05$, $n = 3$ per group).
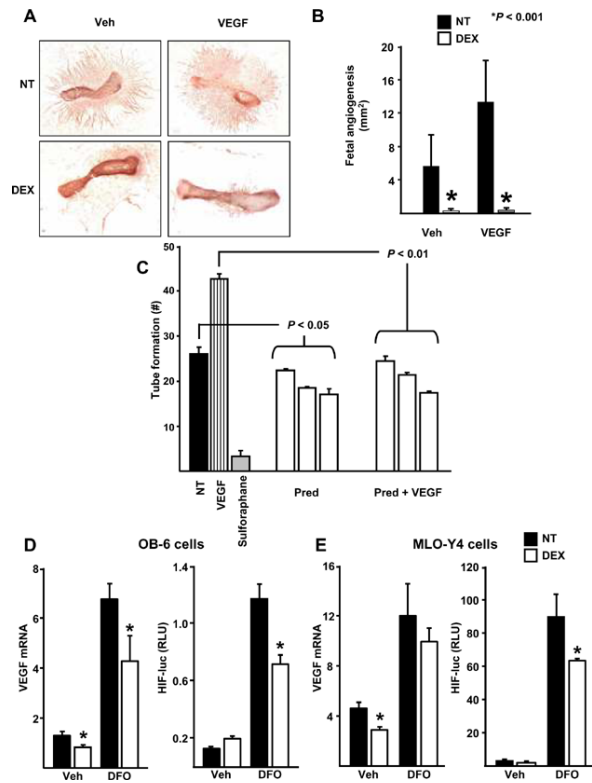
Figure 5.
Bone vasculature decreases with prednisolone administration. Representative images of vertebrae and femora after perfusion with lead chromate administered to 8-month-old female C57BL/6 mice after 28 days of placebo (**A and C**) or prednisolone (**B and D**) administration (*n* = 5 per group). Scale bars: 1 mm. Comparisons of the vertebral blood vessel volume (**E**) and surface area (**F**) in mice receiving placebo (white bars) or prednisolone (pred, grey bars) are shown. * $P < 0.05$. Data indicate the mean ± SD. Representative photomicrographs of immunostaining for von Willebrand factor in sections of cancellous vertebral bone taken from the 8-month-old C57BL/6 mice after placebo (**G**) or prednisolone (**H**). Prednisolone reduced the vascularity by an average of 74.5%. Scale bars: 10 um. The arrow in (**G**) points to ring-shapes typical of cross-sections of blood vessels.

Figure 6.
Preservation of bone lacunar-canalicular fluid, vascular volume, and vascular surface area in 21-month-old OG2-11β-HSD2 (black bars) compared to wild-type mice (white bars). Comparison of solute transport through the vertebral lacunar-canalicular system of male animals is shown in (**A**) and representative photomicrographs are shown in (**B**). Scale bars: 10 um. Comparisons of vertebral (**C, D**) and femoral (**F, G**) blood vessels after perfusion with lead chromate and representative μCT images from female animals (**E**). Scale bars: 1 mm. Data represent the mean ± SD. * $P <0.05$, ** $P <0.02$, *** $P <0.002$. ($n = 6$ to 11 per group. For measurements of procion red fluorescence and vertebral vessels, $n = 3$ per group). Representative photomicrographs of immunostaining for von Willebrand factor in sections of cancellous vertebral bone are shown in (**H**). The 21-month-old transgenics had an average of 77.8% greater vascular staining as compared with the similarly aged wild-type mice. Scale bars: 10 um. The arrow points to a longitudinal section of blood vessel.

Figure 7.
Glucocorticoids inhibit angiogenesis and interfere with VEGF message and action. Fetal metatarsal endothelial sprouting with or without added VEGF was inhibited by 10–8 M dexamethasone (DEX) in wild-type animals (**A, B**). (n = 10 to 12 per group). Prednisolone decreases tube-like structure formation by cultured human umbilical vein endothelial cells (**C**). (NT) indicates no treatment, (VEGF) is vascular endothelial growth factor, (PRED) is 10 to 1000 nM of prednisolone, and sulforaphane is a negative control that suppresses endothelial cell proliferation. In OB-6 osteoblastic cells, 10–8 M DEX decreased basal as well as desferrioxamine (DFO)-stimulated VEGF mRNA levels and decreased DFO-stimulated HIF1α expression (**D**). In MLO-Y4 osteocytic cells, 10–8 M DEX also decreased basal VEGF mRNA levels and DFO-stimulated HIF1α expression (**E**). Data represent the mean ± SD. * $P < 0.05$.